Bulletin of the Seismological Society of America. Vol. 57, No. 3, pp. 477–499. June, 1967

REFLECTION AND TRANSMISSION FROM A PLANE LAYERED CORE-MANTLE BOUNDARY

By Ta-Liang Teng

ABSTRACT

A class of transfer functions in terms of layer matrices is derived, giving the transmission and reflection of plane harmonic *P* or *S* waves incident from either side of a plane layered core-mantle boundary. A computer program coded in complex arithmetic for the IBM 7094 is used to evaluate these functions. Numerical values obtained from five suggested models of the core-mantle boundary are compared and discussed. The aim is to formulate the method, and to establish some general guide, for the studies of the structure of the core-mantle boundary and the attenuation of seismic waves inside the core.

Introduction

Previously, Gutenberg (1959) had proposed that there is a slight decrease in velocity at the base of the mantle (Region D″). The standard solutions for the lower few hundred km of the mantle also suggest that it is at least "mildly inhomogeneous" (Bullen, 1963). Two recent studies, with different approaches, have lent further support to the earlier speculations. On the one hand, from the disagreement between a number of theoretical and observed free periods of the earth's spheroidal oscillation, Dorman *et al* (1966) have raised some doubt about the sharpness of the core-mantle boundary. They have noted that this disagreement can be reconciled by postulating a slightly larger core surrounded by a thin soft layer at the base of the mantle. On the other hand, Phinney and Alexander, 1966; also Alexander and Phinney, 1966 using compressional waves from large earthquakes observed deep inside the shadow zone, calculated spectral ratios and interpreted them in terms of a diffraction theory which they advanced to include a multilayered core-mantle geometry. Their analysis suggested that a layer at the base of the mantle with thickness in the approximate range 30–160 km would fit their data.

The present study makes use of the core phases and interprets them in terms of reflection and transmission at a plane layered core-mantle boundary. This approach is encouraged by the usefulness of the crustal transfer functions in the studies of layered crustal structure (Haskell, 1960, 1962; Phinney, 1964; Fernandez, 1965; among others), and this has recently been attempted by Kanamori (1966). Using spectrums of short-period P and PcP waves, he designed an experiment to measure the Q of the mantle, and at the same time to investigate a possible transitional layer at the core-mantle boundary. Since a short time window ($\sim$5 sec) was used, he was able to measure Q and avoid the complexity due to reflections from a possible layered core-mantle boundary. On the other hand, just because a narrow time window can not adequately include the later arrivals from reverberations caused by the layered structure, his data is not sensitive for the detection of a transitional layer. This insensitivity can also be demonstrated in the frequency domain. If one convolves the core-mantle transfer function with a function corresponding to the

narrow time window, the resulting slowly varying function would give no clear characteristics by which a transitional core-mantle structure can be distinguished from a sharp one.

In order to broaden the application of the transfer function technique to various core phases, the present study first derives a complete class of the complex transfer functions. Both transmission and reflection from *P*-, *SV*-, and *SH*-type incident plane waves at the plane layered core-mantle boundary are considered. A computer program is prepared to evaluate this class of complex transfer functions. Numerical values of these functions for five suggested models of the core-mantle boundary are obtained and they are discussed within the framework of the following questions:

(1) for an assumed structure of the core-mantle boundary, what effects on core phases can be expected and which core phases are more sensitive to the layered structure?

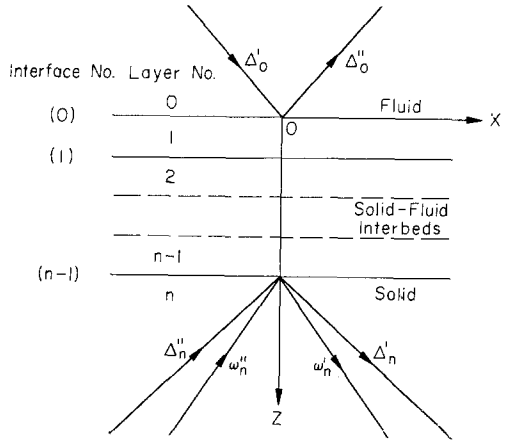

FIG. 1. Geometry of the problem of plane-wave transmission and reflection at a layered boundary.

(2) at what epicentral distances do these effects become more pronounced?

(3) what frequency bands (or records from what instruments) are most suitable to detect these effects?

(4) what window length is best suitable for a study of the core-mantle boundary?

In addition, the above numerical results have also defined the regions (in terms of epicentral distances, frequency bands, and types of core phases) in which the aforementioned effects become small. Consequently, even without detailed knowledge about the core-mantle boundary, one can still make good use of certain core phases to study the attenuation of the earth, particularly the portion inside the core.

THEORY

Consider an infinite space (Figure 1) composed of an upper fluid half-space, a lower solid half-space, and, in between, a number of arbitrarily interbedded solid and fluid layers. Number the fluid half-space the zeroth layer which rests on the zeroth interface, and so on down with the $(n-1)^{\text{th}}$ interface overlying the n^{th} layer, or the solid half-space. All interfaces are parallel.

Continuity of two displacement components and two stress components at each solid-solid interface, and of vertical displacement and normal stress at either solid-fluid or fluid-fluid interface give rise to the following transformations:

$$\begin{bmatrix} \Delta_n' + \Delta_n'' \\ \Delta_n' - \Delta_n'' \\ \omega_n' - \omega_n'' \\ \omega_n' + \omega_n'' \end{bmatrix} = E_n^{-1} A \begin{bmatrix} \dot{u}_r/c \\ \dot{w}_0/c \\ \sigma_0 \\ 0 \end{bmatrix} \tag{1}$$

where

Δ_n , ω_n = the dilatational and rotational amplitudes of P and SV waves in the solid half-space. The single primes represent down-going waves and the double primes represent up-going waves.

E_n^{-1} = the matrix defined by Haskell (1953, equations 2–16).

$\dot{u}_r$ = the horizontal particle velocity at the first solid-fluid interface above the solid half-space.

$\dot{w}_0$ = the vertical particle velocity at the zeroth interface.

σ_0 = the normal stress at the zeroth interface.

c = apparent horizontal velocity.

A is a product of $n - 1$ matrices of the form a_m for a solid layer and a_m' for a fluid layer. The elements of a_m are given in Haskell (1953, p. 21), and a_m' has the form (see Appendix A)

$$a_m' = \begin{bmatrix} 1 & 0 & 0 & 0 \\ 0 & \cos P_m & ir_{\alpha_m}(\rho_m c^2)^{-1} \sin P_m & 0 \\ 0 & i\rho_m c^2 r_{\alpha_m}^{-1} \sin P_m & \cos P_m & 0 \\ 0 & 0 & 0 & 1 \end{bmatrix} \tag{2}$$

where

ρ_m = density

$$r_{\alpha_m} = \begin{cases} [(c/\alpha_m)^2 - 1]^{1/2} & c > \alpha_m \\ -i\,[1 - (c/\alpha_m)^2]^{1/2} & c < \alpha_m \end{cases}$$

$P_m = k r_{\alpha_m} d_m$

$k = \omega/c$

d_m = thickness.

As an example, if $n = 5$, there are four layers between the two half-spaces. Let layer 1, 2, 3, and 4 be fluid, solid, fluid and solid respectively. Then A takes the following form

$$A = a_4 a_3' a_2 a_1'$$

For the fluid half space, the vector $(0, \dot{w}_0/c, \sigma_0, 0)$ and the dilatations Δ_0' and Δ_0'' are related by (see Appendix A)

$$\begin{bmatrix} 0 \\ \dfrac{\dot{w}_{-1}}{c} \\ \sigma_{-1} \\ 0 \end{bmatrix} = E_0' \begin{bmatrix} \Delta_0' + \Delta_0'' \\ \Delta_0' - \Delta_0'' \\ 0 \\ 0 \end{bmatrix} \tag{3}$$

where

$\dot{w}_{-1}$ = the vertical particle velocity in the fluid half-space
σ_{-1} = the normal stress in the fluid half-space

$$E_0' = \begin{bmatrix} 0 & 0 & 0 & 1 \\ 0 & -(\alpha_0/c)^2 r_{\alpha_0} & 0 & 0 \\ \rho_0 \alpha_0^2 & 0 & 0 & 0 \\ 0 & 0 & 1 & 0 \end{bmatrix}. \tag{4}$$

Continuity of vertical particle velocity and normal stress at the zeroth interface results from (1) and (3) in the following relations

$$\begin{aligned} \Delta_n' + \Delta_n'' &= J_{11}\frac{\dot{u}_r}{c} + J_{12}\frac{\dot{w}_0}{c} + J_{13}\sigma_0 \\ \Delta_n' - \Delta_n'' &= J_{21}\frac{\dot{u}_r}{c} + J_{22}\frac{\dot{w}_0}{c} + J_{23}\sigma_0 \\ \omega_n' - \omega_n'' &= J_{31}\frac{\dot{u}_r}{c} + J_{32}\frac{\dot{w}_0}{c} + J_{33}\sigma_0 \\ \omega_n' + \omega_n'' &= J_{41}\frac{\dot{u}_r}{c} + J_{42}\frac{\dot{w}_0}{c} + J_{43}\sigma_0 \\ \Delta_0' + \Delta_0'' &= \sigma_0/(\rho_0\alpha_0^2) \\ \Delta_0' - \Delta_0'' &= -\dot{w}_0 c/(\alpha_0^2 r_{\alpha_0}) \end{aligned} \tag{5}$$

where

$$(J_{ij}) = J = E_n^{-1}A. \tag{6}$$

This system of linear equations is used to solve for the reflection and transmission coefficients for different incident wave types from either half-space.

Incident P waves from solid half space. Setting $\Delta_0'' = \omega_n'' = 0$ and eliminating $\dot{u}_r$, $\dot{w}_0$, σ_0 from (5), we find [1] *P-P* reflection coefficient, S_r^{PP}, due to a *P*-wave

incident from the solid half-space. (The same expression has been given by Kanamori, 1966).

$$S_r^{PP} = \frac{\Delta_n'}{\Delta_n''} = D^{-1}\{[(J_{12} + J_{22})(J_{31} - J_{41}) - (J_{11} + J_{21})(J_{32} - J_{42})]\cdot p + [(J_{13} + J_{23})(J_{31} - J_{41}) - (J_{11} + J_{21})(J_{33} - J_{43})]q\}. \quad (7)$$

[2] P-P transmission coefficient, S_t^{PP}, due to a P-wave incident from the solid half-space

$$S_t^{PP} = \frac{\Delta_0'}{\Delta_n''} = 2D^{-1}(J_{31} - J_{41}). \quad (8)$$

[3] P-SV reflection coefficient, S_r^{PSV}, due to a P-wave incident from the solid half-space

$$S_r^{PSV} = \frac{\omega_n'}{\Delta_n''} = 2D^{-1}[(J_{31}J_{42} - J_{32}J_{41})p + (J_{31}J_{43} - J_{33}J_{41})q] \quad (9)$$

where

$$D = [-(J_{11} - J_{21})(J_{32} - J_{42}) + (J_{12} - J_{22})(J_{31} - J_{41})]p + [-(J_{11} - J_{21})(J_{33} - J_{43}) + (J_{13} - J_{23})(J_{31} - J_{41})]q$$

$$p = (\alpha_0/c)^2 r_{\alpha_0}$$

$$q = \rho_0 \alpha_0^2.$$

Incident SV waves from solid half-space. Setting $\Delta_n'' = \Delta_0' = 0$ and eliminating $\dot{u}_r$, $\dot{w}_0$, σ_0 from (5), we find [4] SV-SV reflection coefficient, S_r^{SVSV}, due to an SV-wave incident from the solid half-space

$$S_r^{SVSV} = \frac{\omega_n'}{\omega_n''} = D^{-1}\{[(J_{21} - J_{11})(J_{32} + J_{42}) + (J_{12} - J_{22})(J_{31} + J_{41})]p + [(J_{21} - J_{11})(J_{33} + J_{43}) + (J_{13} - J_{23})(J_{31} + J_{41})]q\} \quad (10)$$

[5] SV-P transmission coefficient, S_t^{SVP}, due to an SV-wave incident from the solid half-space

$$S_t^{SVP} = \frac{\Delta_0''}{\omega_n''} = 2D^{-1}(J_{21} - J_{11}) \quad (11)$$

[6] SV-P reflection coefficient, S_r^{SVP}, due to an SV-wave incident from the solid half-space

$$S_r^{SVP} = \frac{\Delta_n'}{\omega_n''} = 2D^{-1}[(J_{12}J_{21} - J_{11}J_{22})p + (J_{13}J_{21} - J_{11}J_{23})q]. \quad (12)$$

Incident SH waves from the solid half-space. [7] *SH-SH* reflection coefficient, S_r^{SHSH}

$$S_r^{SHSH} = \frac{\mu_n r_{\beta_n} A_{11} - A_{21}}{\mu_n r_{\beta_n} A_{11} + A_{21}} \tag{13}$$

where

$$r_{\beta_n} = \begin{cases} [(c/\beta_n)^2 - 1]^{1/2} & c > \beta_n \\ -i[1 - (c/\beta_n)^2]^{1/2} & c < \beta_n \end{cases}$$

μ_n = rigidity of the solid half-space

$A_{ij} = \prod_{m=1}^{n-1} a_m$, and a_m is given by equation 3 of Haskell (1960).

The amplitude part of (13) is trivial: $| S_r^{SHSH} | \equiv 1$; as required by energy conservation, total reflection must occur at the first solid-fluid interface.

Incident P waves from the fluid half-space. Similarly, setting $\Delta_n'' = \omega_n'' = 0$ and eliminating $\dot{u}_r'$, $\dot{w}_0$, σ_0 from (5), we find [8] *P-P* reflection coefficient, F_r^{PP}, due to a *P*-wave incident from the fluid half-space

$$F_r^{PP} = \frac{\Delta_0''}{\Delta_0'} = D^{-1}\{[-(J_{11} - J_{21})(J_{32} - J_{42}) + (J_{12} - J_{22})(J_{31} - J_{41})]p - [-(J_{11} - J_{21})(J_{33} - J_{43}) + (J_{13} - J_{23})(J_{31} - J_{41})]q\} \tag{14}$$

[9] *P-P* transmission coefficient, F_t^{PP}, due to a *P*-wave incident from the fluid half-space

$$F_t^{PP} = \frac{\Delta_n'}{\Delta_0'} = 2pqD^{-1}[(J_{31} - J_{41})(J_{12}J_{23} - J_{13}J_{22}) + (J_{32} - J_{42})(J_{13}J_{21} - J_{11}J_{23}) + (J_{33} - J_{43})(J_{11}J_{22} - J_{12}J_{21})] \tag{15}$$

[10] *P-SV* transmission coefficient, F_t^{PSV}, due to a *P*-wave incident from the fluid half-space

$$F_t^{PSV} = \frac{\omega_n'}{\Delta_0'} = 2pqD^{-1}[(J_{11} - J_{21})(J_{33}J_{42} - J_{32}J_{43}) + (J_{12} - J_{22})(J_{31}J_{43} - J_{33}J_{41}) + (J_{13} - J_{23})(J_{32}J_{41} - J_{31}J_{42})]. \tag{16}$$

Energy Relationships

For an arbitrary number of plane parallel layers, the energy flow rate ϵ_{n-1}, across the $(n-1)^{\text{th}}$ interface (Figure 1) can be calculated by

$$\epsilon_{n-1} = R(\dot{u}_{n-1}\tau_{n-1}^* + \dot{w}_{n-1}\sigma_{n-1}^*) \tag{17}$$

where R indicates the real part of the complex quantity that follows. This can be shown to equal (Haskell, 1962).

$$\epsilon_{n-1} = (\rho_n\alpha_n^4/c)(|\Delta_n''|^2 - |\Delta_n'|^2)R(r_{\alpha_n}) + 4(\rho_n\beta_n^4/c)(|\omega_n''|^2 - |\omega_n'|^2)r_{\beta_n}. \tag{18}$$

Likewise, the energy flow rate, ϵ_{-1}, across the zeroth interface can be calculated by

$$\epsilon_{-1} = R(\dot{u}_{-1}\tau_{-1}^{*} + \dot{w}_{-1}\sigma_{-1}^{*}).$$

If the zeroth layer is fluid

$$\epsilon_{-1} = R(\dot{w}_{-1}\sigma_{-1}^{*}). \tag{19}$$

From (3) and (4) we have

$$\begin{aligned} \dot{w}_{-1} &= -(\alpha_0^{2} r_{\alpha_0}/c)(\Delta_0' - \Delta_0'') \\ \sigma_{-1}^{*} &= \rho_0\alpha_0^{2}(\Delta_0'^{*} + \Delta_0''^{*}). \end{aligned} \tag{20}$$

Putting (20) into (19), we find

$$\begin{aligned} \epsilon_{-1} = -(\rho_0\alpha_0^{4}/c)\{&R[r_{\alpha_0}(|\Delta_0'|^2 - |\Delta_0''|^2)] \\ &+ R[r_{\alpha_0}(\Delta_0'\Delta_0''^{*} - \Delta_0'^{*}\Delta_0'')]\}. \end{aligned} \tag{21}$$

Here, $(|\Delta_0'|^2 - |\Delta_0''|^2)$ is always real, and $(\Delta_0'\Delta_0''^{*} - \Delta_0'^{*}\Delta_0'')$ is always pure imaginary. For $c > \alpha_0$, r_{α_0} is real and the second term in the square brackets vanishes. But for $c < \alpha_0$, r_{α_0} is pure imaginary, the finiteness of the displacements at infinity requires that $\Delta_0'' = 0$, therefore, both terms in the square brackets vanish. This latter case corresponds to a total reflection at the zeroth interface across which no energy transmits, or $\epsilon_{-1} = 0$. The former case is more interesting, corresponding to wave reflection and transmission. The partition of energy among these reflected and transmitted waves is to be discussed in the following.

If the medium is non-dissipative, by the law of energy conservation we have

$$\begin{aligned} (\rho_0\alpha_0^{4}/c)(|\Delta_0'|^2 - |\Delta_0''|^2) r_{\alpha_0} = {} & (\rho_n\alpha_n^{4}/c)(|\Delta_n''|^2 - |\Delta_n'|^2) R(r_{\alpha_n}) \\ & + 4(\rho_n\beta_n^{4}/c)(|\omega_n''|^2 - |\omega_n'|^2)\, r_{\beta_n}. \end{aligned} \tag{22}$$

For the P-type incident waves from the solid half-space, ($\Delta_0' = \omega_n'' = 0$) the partition of energy among the reflected and transmitted P and S waves is given from (7), (8) and (9) by

$$\begin{aligned} E_{S_r}^{PP} = |\Delta_n'/\Delta_n''|^2 = |D^{-1}\{&[(J_{12} + J_{22})(J_{31} - J_{41}) \\ &- (J_{11} + J_{21})(J_{32} - J_{42})]p + [(J_{13} + J_{23})(J_{31} - J_{41}) \\ &- (J_{11} + J_{21})(J_{33} - J_{43})]q\}|^2 \end{aligned} \tag{23}$$

$$\begin{aligned} E_{S_t}^{PP} &= [(\rho_0\alpha_0^{4} r_{\alpha_0})/(\rho_n\alpha_n^{4} r_{\alpha_n})]\,|\Delta_0''/\Delta_n''|^2 \\ &= 4[(\rho_0\alpha_0^{4} r_{\alpha_0})/(\rho_n\alpha_n^{4} r_{\alpha_n})]\,|D^{-1}(J_{31} - J_{41})|^2 \end{aligned} \tag{24}$$

$$E_{S_r}^{PSV} = 4[(\beta_n {}^4 r_{\beta_n})/(\alpha_n {}^4 r_{\alpha_n})] \mid \omega_n'/\Delta_n'' \mid^2$$

$$= 16[(\beta_n {}^4 r_{\beta_n})/(\alpha_n {}^4 r_{\alpha_n})] \mid D^{-1}[(J_{31}J_{42} - J_{32}J_{41})p + (J_{31}J_{43} - J_{33}J_{41})q] \mid^2. \quad (25)$$

If the incident waves are of SV type from the solid half-space, ($\Delta_0' = \Delta_n'' = 0$), the partition of energy among the reflected and transmitted P and S waves is given from (10), (11), and (12) by

$$E_{S_r}^{SVSV} = \mid \omega_n'/\omega_n'' \mid^2 = \mid D^{-1}\{[(J_{21} - J_{11})(J_{32} + J_{42}) + (J_{12} - J_{22})(J_{31} + J_{41})]p + [(J_{21} - J_{11})(J_{23} + J_{43}) + (J_{13} - J_{23})(J_{31} + J_{41})]q\} \mid^2 \quad (26)$$

$$E_{S_t}^{SVP} = [(\rho_0\alpha_0 {}^4 r_{\alpha_0})/(4\rho_n\beta_n {}^4 r_{\alpha_n})] \mid \Delta_0''/\omega_n'' \mid^2$$

$$= [(\rho_0\alpha_0 {}^4 r_{\alpha_0})/(\rho_n\beta_n {}^4 r_{\beta_n})] \mid D^{-1}(J_{21} - J_{11}) \mid^2 \quad (27)$$

$$E_{S_r}^{SVP} = [(\alpha_n {}^4 r_{\alpha_n})/(4\beta_n {}^4 r_{\beta_n})] \mid \Delta_n'/\omega_n'' \mid^2$$

$$= [(\alpha_n {}^4 r_{\alpha_n})/(\beta_n {}^4 r_{\beta_n})] \mid D^{-1}[(J_{12}J_{21} - J_{11}J_{22})p + (J_{13}J_{21} - J_{11}J_{23})q] \mid^2. \quad (28)$$

If the incident waves are of P type from the fluid half-space, $\omega_n' = \Delta_n'' = 0$, the partition of energy among the reflected P and the transmitted P and S waves is given from (14), (15), and (16) by

$$E_{F_r}^{PP} = \mid \Delta_0''/\Delta_0' \mid^2 = \mid D^{-1}\{[-(J_{11} - J_{21})(J_{32} - J_{42}) + (J_{11} - J_{22}) \cdot (J_{31} - J_{41})]p - [-(J_{11} - J_{21})(J_{33} - J_{43}) + (J_{13} - J_{23})(J_{31} - J_{41})]q\} \mid^2 \quad (29)$$

$$E_{F_t}^{PP} = [(\rho_n\alpha_n {}^4 r_{\alpha_n})/(\rho_0\alpha_0 {}^4 r_{\alpha_0})] \mid \Delta_n'/\Delta_0' \mid^2$$

$$= 4[(\rho_n\alpha_n {}^4 r_{\alpha_n})/(\rho_0\alpha_0 {}^4 r_{\alpha_0})] \mid pqD^{-1} \cdot [(J_{31} - J_{41})(J_{12}J_{23} - J_{13}J_{22}) + (J_{32} - J_{42})(J_{13}J_{21} - J_{11}J_{23}) + (J_{33} - J_{43})(J_{11}J_{22} - J_{12}J_{21})] \mid^2 \quad (30)$$

$$E_{F_t}^{PS} = 4[(\rho_n\beta_n{}^4 r_{\beta_n})/(\rho_0\alpha_0{}^4 r_{\alpha_0})] \mid \omega_n'/\Delta_0' \mid^2$$

$$= 16[(\rho_n\beta_n{}^4 r_{\beta_n})/(\rho_0\alpha_0{}^4 r_{\alpha_0})] \mid pqD^{-1}[(J_{11} - J_{21})(J_{33}J_{42} - J_{32}J_{43})$$

$$+ (J_{12} - J_{22})(J_{31}J_{43} - J_{33}J_{41}) + (J_{13} - J_{23})$$

$$\cdot (J_{32}J_{41} - J_{31}J_{42})] \mid^2. \quad (31)$$

The law of energy conservation (22) can be, therefore, written in more explicit form:

$$\begin{aligned} E_{S_r}^{PP} + E_{S_r}^{PSV} + E_{S_t}^{PP} &= 1 \\ E_{S_r}^{SVSV} + E_{S_r}^{SVP} + E_{S_t}^{SVP} &= 1 \\ E_{F_r}^{PP} + E_{F_t}^{PP} + E_{F_t}^{PSV} &= 1. \end{aligned} \quad (32)$$

It can also be shown (Appendix B) that for equal values of c the following relations exist:

$$\begin{aligned} E_{S_t}^{PP}(c) &= E_{F_t}^{PP}(c) \\ E_{S_r}^{PSV}(c) &= E_{S_r}^{SVP}(c) \end{aligned} \quad (33)$$

and

$$E_{S_t}^{SVP}(c) = E_{F_t}^{PSV}(c).$$

By (32) and (33) it is therefore only necessary to calculate three distinct E functions and the other six can be obtained through elementary operations. (33) remains true if both half spaces are solid.

Numerical Results

A Fortran program has been written in complex arithmetic for an IBM 7094 to evaluate the functions in equations (7) to (16). Numerical results have been obtained for a number of models, whose layer parameters are given in Table 1. These results provide a useful guidance in designing seismological experiments in the study of the earth's deep interior. From these numerical results based on a postulated model of the core-mantle boundary, one would be able to expect the effects of the corresponding transfer functions on various core phases. Conversely, by examining these effects, it becomes simple to select the most desirable kind of core phase data, in terms of wave types, recording frequency bands, and epicentral distances, which would lead to the best experimental results.

In Figures 2, and 3, comparisons are made between several transfer functions computed for the five models given in Table 1. These curves, plotted at fixed incident

TABLE 1

MODELS OF CORE-MANTLE BOUNDARY†

Model No.	Layer No.	Thickness km	α km/sec	β km/sec	ρ gr/cm^3
1	0	∞	8.040	0.000	10.060
	1	20.00	13.680	7.200	5.355
	2	80.00	13.700	7.225	5.325
	3	∞	13.700	7.250	5.300
2	0	∞	8.150	0.000	9.400
	1	18.00	13.720	7.195	5.675
	2	20.00	13.710	7.200	5.665
	3	20.00	13.700	7.205	5.655
	4	20.00	13.690	7.215	5.645
	5	∞	13.680	7.220	5.640
3	0	∞	8.150	0.000	9.400
	1	11.00	10.200	5.200	6.200
	2	13.00	11.600	6.100	5.670
	3	12.00	13.000	6.840	5.660
	4	∞	13.690	7.210	5.650
4	0	∞	8.300	0.000	9.500
	1	30.00	10.000	2.800	6.700
	2	∞	13.600	7.500	5.500
5	0	∞	8.300	0.000	9.500
	1	100.00	13.300	4.800	6.700
	2	∞	13.600	7.500	5.500

† The interface between the zeroth and the first layers corresponds to a depth of 2898 km. The model number refers to:

(1) Gutenberg—Bullard I (Landisman *et al*, 1965)
(2) Standard model (Dorman *et al*, 1966)
(3) Model R 1 (Dorman *et al*, 1966)
(4) Model 94 (Phinney and Alexander, 1966)
(5) Model 81 (Phinney and Alexander, 1966)

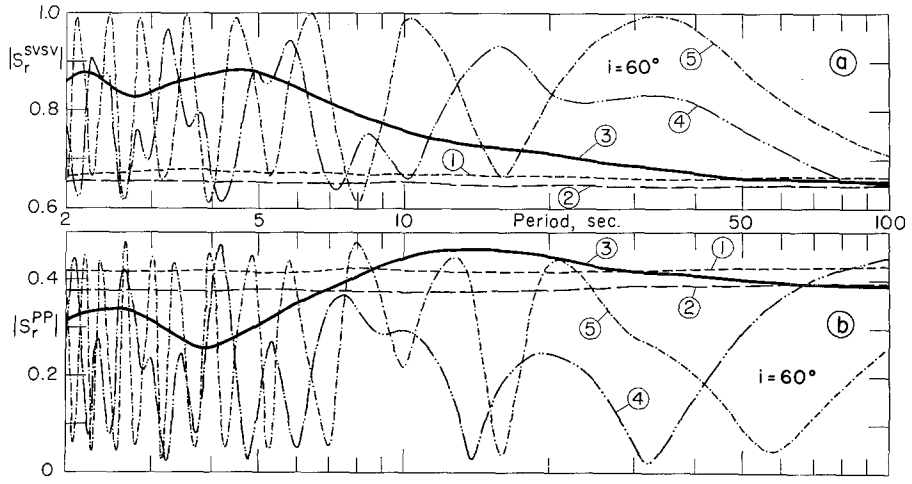

FIG. 2. Comparisons between the five core-mantle boundary models given in Table 1. (a) Amplitude ratio for the reflected S wave due to an S-wave incident in the mantle against the core. (b) Amplitude ratio for the reflected P wave due to a P-wave incident in the mantle against the core.

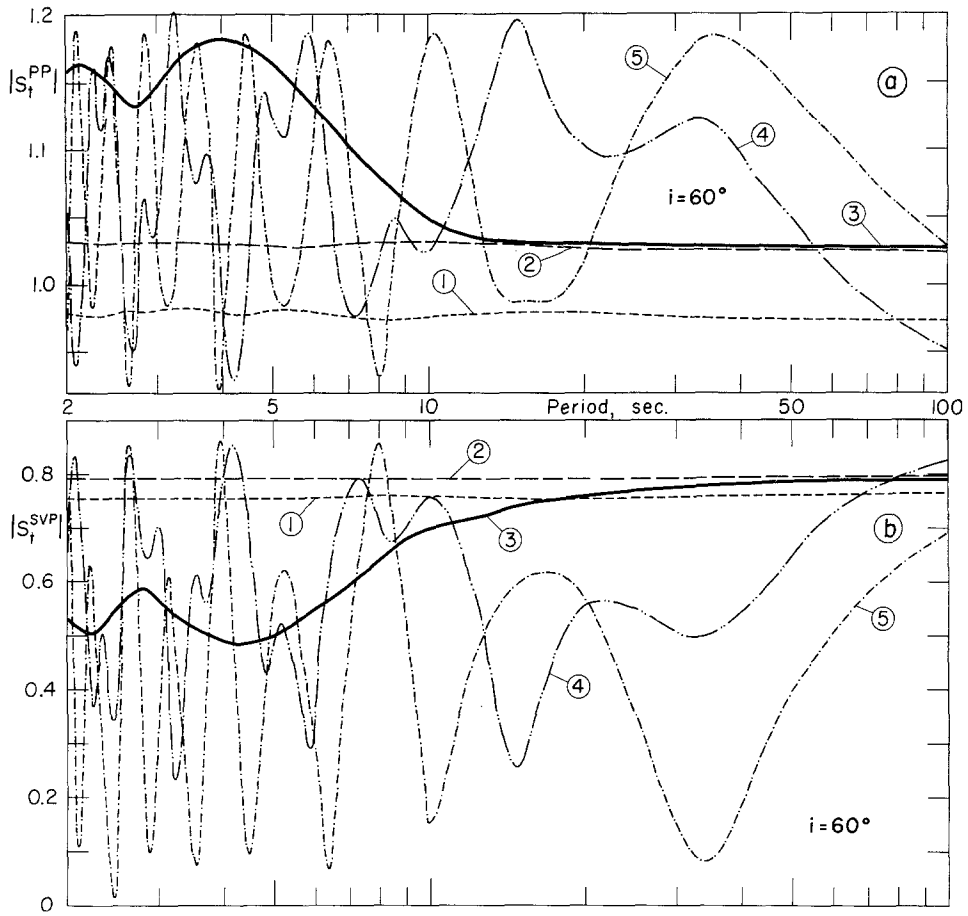

FIG. 3. Comparisons between the five core-mantle boundary models given in Table 1. (a) Amplitude ratio for the transmitted P wave due to a P-wave incident in the mantle against the core. (b) Amplitude ratio for the transmitted P wave due to an S-wave incident in the mantle against the core.

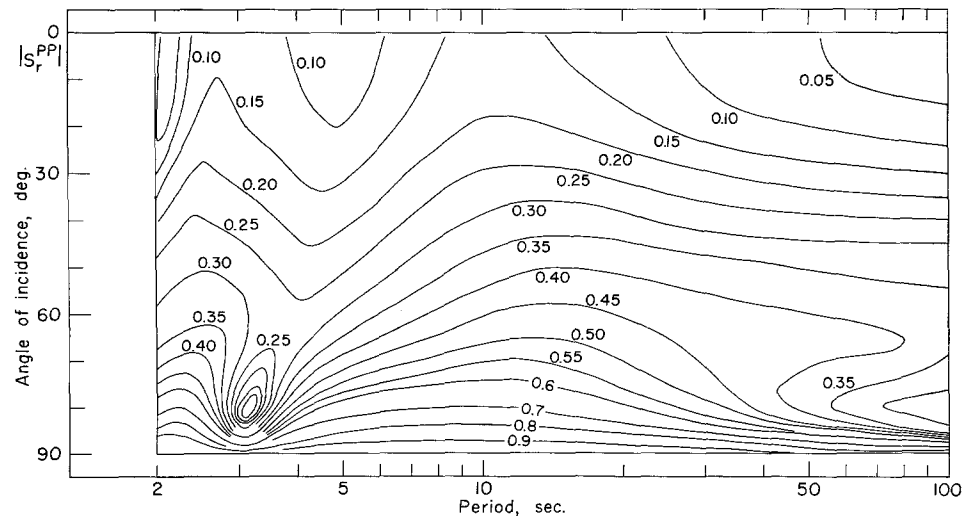

FIG. 4. Amplitude ratio for the reflected P wave due to a P-wave incident in the mantle against the core.

angle $i = 60°$, indicate the degree of distortion a wave signal would have suffered from reflecting off or transmitting through such a layered model. Clearly, the function $S_r^{SV,V}$ is associated with ScS, likewise S_r^{PP} with PcP, S_t^{PP} with PKP, and

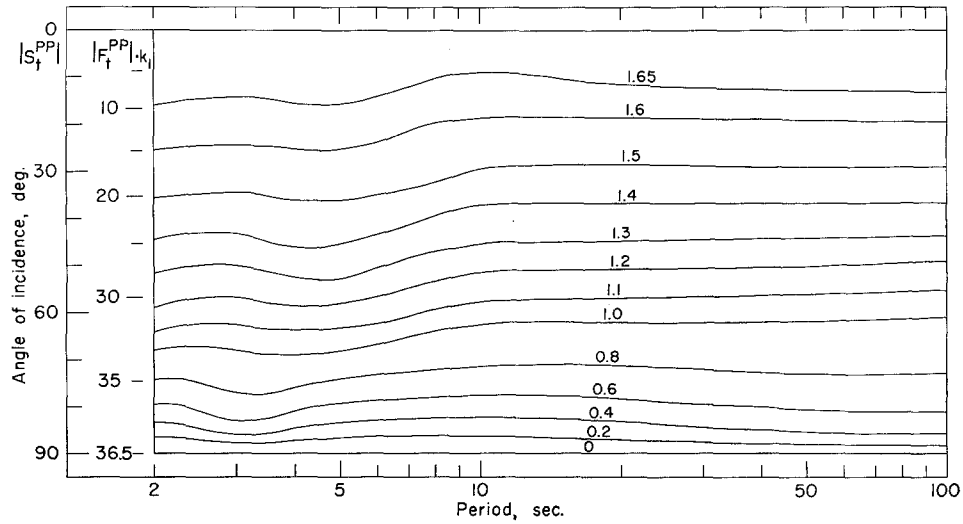

FIG. 5. Amplitude ratio for the transmitted P wave due to a P-wave incident in the mantle (core) against the core (mantle). $k_1 = (\rho_n \alpha^4 r_{\alpha_n})/(\rho_0 \alpha_0^4 r_{\alpha_0})$, its numerical values are shown in Figure 9.

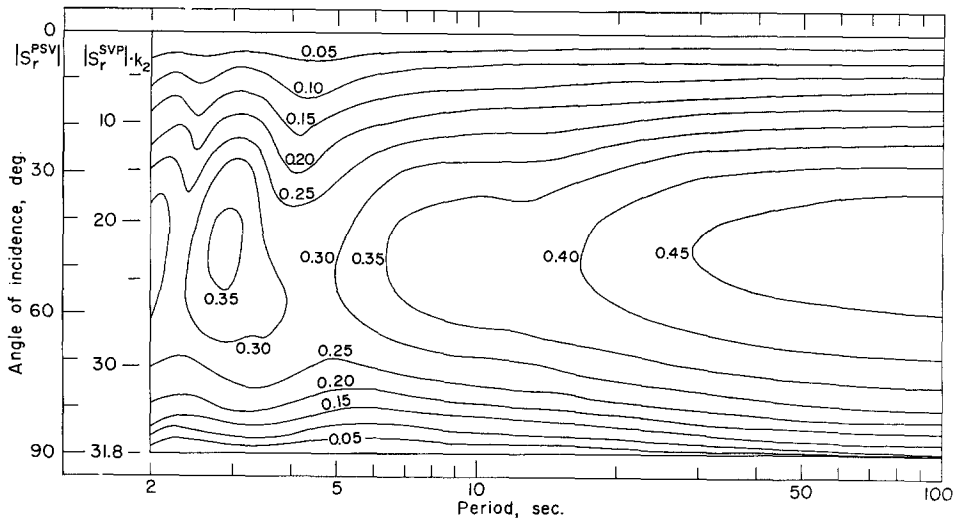

FIG. 6. Amplitude ratio for the reflected $S(P)$ wave due to a $P(S)$-wave incident in the mantle against the core. $k_2 = (\alpha_n^4 r_{\alpha_n})/(4\beta_n^4 r_{\beta_n})$, its numerical values are shown in Figure 9.

S_t^{SP} with SKS, etc. Over the entire plotted period range, these functional forms for model 1 and model 2 hardly differ from those for the case of two half-spaces in contact. To discriminate model 1 from model 2, one would have to go to much higher frequencies and shallower incident angles. Between 10 and 100 seconds period range,

it is difficult with the present capability of the long-period recording instruments to separate model 3 from the previous two models. However, this separation becomes possible for periods shorter than ten seconds. Among wave types, *PcP* appears to be

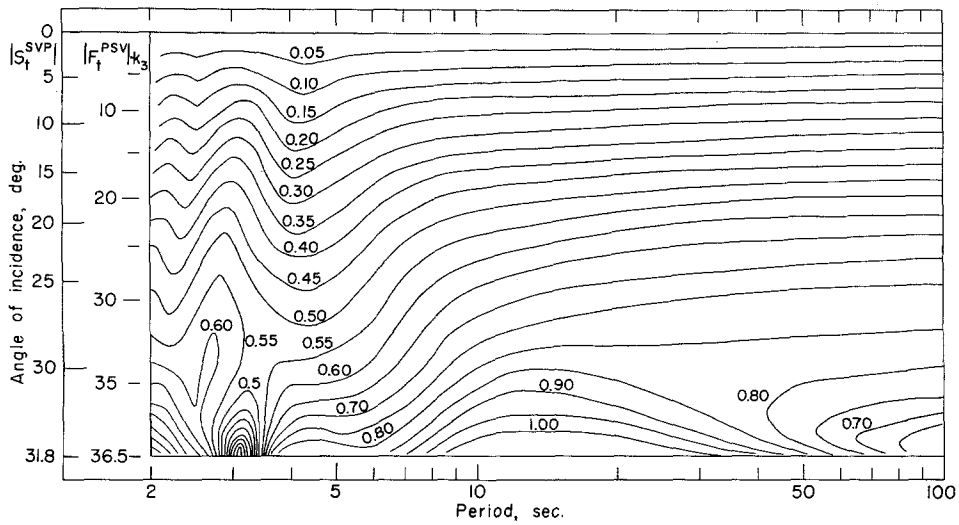

FIG. 7. Amplitude ratio for the transmitted $P(S)$ wave due to an $S(P)$-wave incident in the mantle (core) against the core (mantle). $k_2 = (2\rho_n\beta_n{}^4 r_{\beta_n})/(\rho_0\alpha_0{}^4 r_{\alpha_0})$, its numerical values are shown in Figure 9.

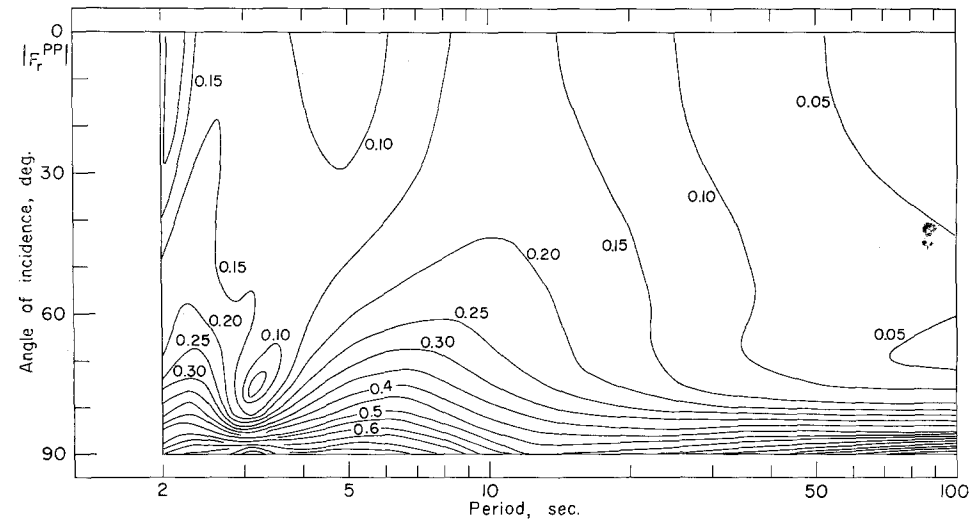

FIG. 8. Amplitude ratio for the reflected P wave due to a P-wave incident in the core against the mantle.

more desirable for this purpose, because the function $S_r{}^{PP}$ has the largest variation ($\sim$40%) over the period range of 2 to 10 seconds. All amplitude functions for model 4 and model 5 have distinctive characteristics. Therefore, all core phases except those with steep incident angles can be conveniently used to find out whether the

true model of the core mantle boundary is closer to model 4 or model 5, or instead to the first three models. Also revealed by these figures are the larger variations of S_r^{PP} and S_t^{SVP} ($>40\%$) as compared to those of S_r^{SVSV} and S_t^{PP} ($<20\%$). These results imply that *PcP* and *SKS* are probably more sensitive to the core-mantle boundary structure while *ScS* and *PKP* are more useful in attenuation studies.

To show the variations of these transfer functions with changing incident angles, we present in Figures 4, 5, 6, 7, and 8, the functions S_r^{PP}, S_t^{PP}, F_t^{PP}, S_r^{PSV}, S_r^{SVP}, S_t^{SVP}, F_t^{PSV} and F_r^{PP} in the form of contour maps. They are computed based on model 3, the associated numerical values of k_1, k_2, and k_3 are presented in Figure 9. The function S_r^{SVSV} is not shown here but it can be obtained easily from these

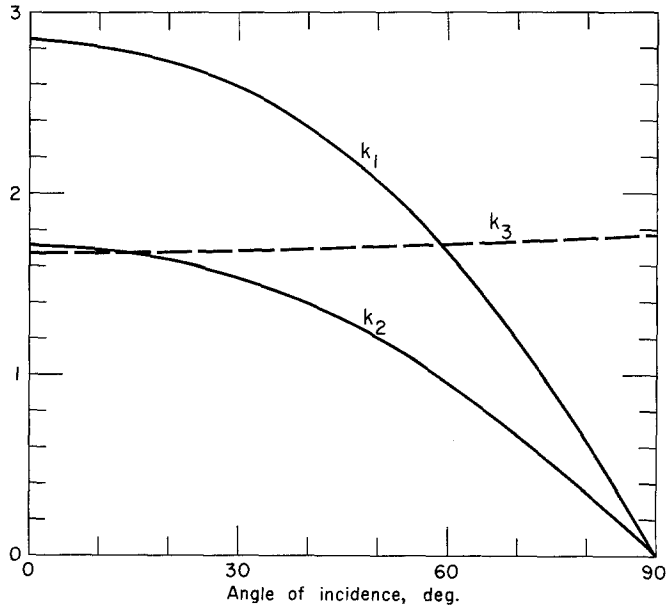

FIG. 9. The conversion constants for Model 3.

figures through the simple relations (32) and (33). These contour maps present a comprehensive picture that is useful in designing experiments. Regions with rough topography can quickly be located which, with reference to travel-time charts and instrumental response curves, simply point out the optimal choice in wave type, epicentral distances and recording instruments for a more effective investigation on the structure. By the same token but with different emphasis, regions with relatively flat topography indicate that the effects of wave transmission and reflection are small and may be neglected under some circumstances.

As it is expected by the scale law of the wavelength, the topography becomes progressively complicated with increasing incident angle and frequency. When the frequency approaches zero, the values of each function approach the right limits which are equivalent to the case of a fluid and a solid half spaces in contact.

APPENDIX A
ON THE FLUID LAYER MATRIX

For solid layers, the matrix E_m relating the motion-stress vector ($\dot{u}_m/c$, $\dot{w}_m/c$, σ_m, τ_m) with the vector ($\Delta_m' + \Delta_m''$, $\Delta_m' - \Delta_m''$, $\omega_m' - \omega_m''$, $\omega_m' + \omega_m''$) across the $(m-1)^{\text{th}}$ interface, and the matrix D_m, connecting the two vectors across the m^{th} layer, are unambiguously given by Haskell (1953, equations 12 and 14). However, as the theory was extended to include fluid layers by setting $\beta_m = 0$, it was found that the matrix E_m becomes singular. This led Haskell to define an *effective* inverse E_m (expressed by F_m^{-1} in equation 6.1) such that the layered matrix a_m (equation 6.3) can be constructed. Haskell (see Dorman, 1962) later pointed out that on setting $\beta_m = 0$, the matrices E_m and D_m lead to overspecified boundary conditions, because only vertical motion and normal stress are continuous across a fluid interface. Using these two boundary equations, Dorman (1962) derived a 2×2 matrix l_m, for fluid layers which properly accounts for the boundary conditions.

It is possible to write a 4×4 matrix for a fluid layer such that, for a sequence of fluid and solid interbeds, dimensions of the layer matrices are consistant throughout in the matrix formulation. In addition to being formally desirable, it also offers obvious convenience in numerical programming.

Since only vertical motion $\dot{w}/c$ and normal stress σ are continuous for a fluid layer, we can think of the two-dimensional motion-stress vector ($\dot{w}/c$, σ) and its associated dilation vector ($\Delta' + \Delta''$, $\Delta' - \Delta''$) as two degenerated four-dimensional vectors (0, $\dot{w}/c$, σ, 0) and ($\Delta' + \Delta'$, $\Delta' - \Delta''$, 0, 0). Our problem then is to find the correct transformations, or matrix operators, which relate the two degenerated vectors across a fluid interface or a fluid layer.

The boundary conditions for the $(m-1)^{\text{th}}$ interface are

$$\dot{w}_{m-1}/c = -(\alpha_m/c)^2 r_{\alpha_m}(\Delta_m' - \Delta_m'')$$

$$\sigma_{m-1} = \rho_m \alpha_m^2 (\Delta_m' + \Delta_m''). \tag{A-1}$$

Corresponding to E_m for a solid interface, define for a fluid interface a 4×4 matrix E_m' such that

$$\begin{bmatrix} 0 \\ \dfrac{\dot{w}_{m-1}}{c} \\ \sigma_m \\ 0 \end{bmatrix} = E_m' \begin{bmatrix} \Delta_m' + \Delta_m'' \\ \Delta_m' - \Delta_m'' \\ 0 \\ 0 \end{bmatrix} \tag{A-2}$$

and

$$E_m' = \begin{bmatrix} 0 & 0 & b_{11} & b_{12} \\ 0 & -(\alpha_m/c)^2 r_{\alpha_m} & b_{13} & b_{14} \\ \rho_m \alpha_m^2 & 0 & b_{15} & b_{16} \\ 0 & 0 & b_{17} & b_{18} \end{bmatrix} \tag{A-3}$$

where $b_{ij}(i = 1, 2, 3, 4; j = 1, 2, \cdots 8)$ are certain functions to be determined. The inverse transformations of (A-1)

$$\begin{aligned} \Delta_m' + \Delta_m'' &= \sigma_{m-1}/\rho_m \alpha_m^2 \\ \Delta_m' - \Delta_m'' &= (c/\alpha_m)^2 r_{\alpha_m}^{-1} \dot{w}_{m-1}/c \end{aligned} \tag{A-4}$$

implies that E_m' cannot be singular. Its inverse $(E_m')^{-1}$ can be written by

$$(E_m')^{-1} = \begin{bmatrix} b_{21} & 0 & (\rho_m \alpha_m^2)^{-1} & b_{22} \\ b_{23} & -(c/\alpha_m)^2 r_{\alpha_m}^{-1} & 0 & b_{24} \\ b_{25} & 0 & 0 & b_{26} \\ b_{27} & 0 & 0 & b_{28} \end{bmatrix}. \tag{A-5}$$

CU/82

Across the n^{th} layer, the transformations are

$$\begin{aligned} \dot{w}_m/c &= -(\alpha_m/c)^2 r_{\alpha_m}[-i(\Delta_m' + \Delta_m'') \sin P_m + (\Delta_m' - \Delta_m'') \cos P_m] \\ \sigma_m &= \rho_m \alpha_m^2[(\Delta_m' + \Delta_m'') \cos P_m - i(\Delta_m' - \Delta_m'') \sin P_m]. \end{aligned} \tag{A-6}$$

Then, corresponding to D_m for a solid layer, define for a fluid layer a 4×4 matrix D_m' such that

$$\begin{bmatrix} 0 \\ \dot{w}_m/c \\ \sigma_m \\ 0 \end{bmatrix} = D_m' \begin{bmatrix} \Delta_m' + \Delta_m'' \\ \Delta_m' - \Delta_m'' \\ 0 \\ 0 \end{bmatrix} \tag{A-7}$$

and

$$D_m' = \begin{bmatrix} 0 & 0 & b_{31} & b_{32} \\ i(\alpha_m/c)^2 r_{\alpha_m} \sin P_m & -(\alpha_m/c)^2 r_{\alpha_m} \cos P_m & b_{33} & b_{34} \\ \rho_m \alpha_m^2 \cos P_m & -i\rho_m \alpha_m^2 \sin P_m & b_{35} & b_{36} \\ 0 & 0 & b_{32} & b_{38} \end{bmatrix}. \tag{A-8}$$

Moreover, a 4×4 fluid layer matrix $a_m' = D_m'(E_m')^{-1}$ can be defined which governs the transformations of the motion-stress vector between layers

$$\begin{bmatrix} 0 \\ \dot{w}_m/c \\ \sigma_m \\ 0 \end{bmatrix} = a_m' \begin{bmatrix} 0 \\ \dot{w}_{m-1}/c \\ \sigma_{m-1} \\ 0 \end{bmatrix} \tag{A-9}$$

by

$$a_m' = \begin{bmatrix} b_{41} & 0 & 0 & b_{45} \\ b_{42} & \cos P_m & ir_{\alpha_m}(\rho_m c^2)^{-1} \sin P_m & b_{46} \\ b_{43} & i\rho_m c^2 r_{\alpha_m}^{-1} \sin P_m & \cos P_m & b_{42} \\ b_{44} & 0 & 0 & b_{48} \end{bmatrix}. \tag{A-10}$$

Since by definition

$$E_m'(E_m')^{-1} = (E_m')^{-1}E_m' = I \tag{A-11}$$

$$a_m' = D_m'(E_m')^{-1} \tag{A-12}$$

(A-11) and (A-12) still do not provide enough independent conditions to uniquely determine the b_{ij}'s. We then further require that when the thickness of a layer approaches zero, the layer matrix a_m' becomes an identity matrix. With this additional condition, it is found and can be verified by direct substitution that

$$b_{12} = b_{17} = b_{26} = b_{27} = b_{32} = b_{37} = b_{41} = b_{48} = 1$$

and all other b_{ij}'s are zero.
We, therefore, obtain the following 4×4 matrices for a fluid layer

$$E_m' = \begin{bmatrix} 0 & 0 & 0 & 1 \\ 0 & -(\alpha_m/c)^2 r_{\alpha_m} & 0 & 0 \\ \rho_m \alpha_m^2 & 0 & 0 & 0 \\ 0 & 0 & 1 & 0 \end{bmatrix} \tag{A-13}$$

$$(E_m')^{-1} = \begin{bmatrix} 0 & 0 & (\rho_m \alpha_m^2)^{-1} & 0 \\ 0 & -(c/\alpha_m)^2 r_{\alpha_m}^{-1} & 0 & 0 \\ 0 & 0 & 0 & 1 \\ 1 & 0 & 0 & 0 \end{bmatrix} \tag{A-14}$$

$$D_m' = \begin{bmatrix} 0 & 0 & 0 & 1 \\ i(\alpha_m/c)^2 r_{\alpha_m} \sin P_m & -(\alpha_m/c)^2 r_{\alpha_m} \cos P_m & 0 & 0 \\ \rho_m \alpha_m{}^2 \cos P_m & -i\rho_m \alpha_m{}^2 \sin P_m & 0 & 0 \\ 0 & 0 & 1 & 0 \end{bmatrix} \tag{A-15}$$

and

$$a_m' = \begin{bmatrix} 1 & 0 & 0 & 0 \\ 0 & \cos P_m & ir_{\alpha_m}(\rho_m c)^{-1} \sin P_m & 0 \\ 0 & i\rho_m c^2 r_{\alpha_m}^{-1} \sin P_m & \cos P_m & 0 \\ 0 & 0 & 0 & 1 \end{bmatrix}. \tag{A-16}$$

Appendix B

In this appendix we shall give proof to the relations in equation (33). We first write

$$E_n^{-1} = (\eta_{ij}) \equiv \begin{bmatrix} -2(\beta_n/\alpha_n)^2 & 0 & (\rho_n \alpha_n{}^2)^{-1} & 0 \\ 0 & c^2(\gamma_{n-1})/\alpha_n{}^2 r_{\alpha_n} & 0 & (\rho_n \alpha_n{}^2 r_{\alpha_n})^{-1} \\ (\gamma_{n-1})/\gamma_n r_{\beta_n} & 0 & -(\rho_n c^2 \gamma_n r_{\beta_n})^{-1} & 0 \\ 0 & 1 & 0 & (\rho_n c^2 \gamma_n)^{-1} \end{bmatrix} \tag{B-1}$$

and note that

$$\eta_{22}\eta_{13} = -\eta_{31}\eta_{24} \tag{B-2}$$

$$\eta_{13} = -\eta_{11}\eta_{44}\,. \tag{B-3}$$

By virtue of the law of energy conservation, the elements of the matrix $A = (A_{ij})$ obey the following identities (Haskell, 1962)

$$A_{11}A_{42} - A_{21}A_{32} + A_{31}A_{22} - A_{41}A_{12} \equiv 0 \tag{B-4}$$

$$A_{21}A_{33} - A_{11}A_{43} + A_{13}A_{41} - A_{23}A_{31} \equiv 0 \tag{B-5}$$

$$A_{12}A_{44} - A_{22}A_{34} + A_{32}A_{24} - A_{42}A_{14} \equiv 0 \tag{B-6}$$

$$A_{13}A_{44} - A_{23}A_{34} + A_{24}A_{33} - A_{14}A_{43} \equiv 0 \tag{B-7}$$

$$A_{11}A_{44} - A_{21}A_{34} + A_{24}A_{31} - A_{14}A_{41} \equiv 1 \tag{B-8}$$

$$A_{22}A_{33} - A_{12}A_{43} + A_{13}A_{42} - A_{23}A_{32} \equiv 1. \tag{B-9}$$

The matrix $J = (J_{ij})$, the elements of which make up our transfer functions, is related to the matrix A by,

$$J_{ij} = \eta_{ik} A_{kj} . \tag{B-10}$$

(**1**) To prove the first relation of (33), it is sufficient to show that

$$\begin{aligned} \frac{c^2}{\rho_n \alpha_n{}^4 r_{\alpha n}} (J_{31} - J_{41}) - [(J_{31} - J_{41})(J_{12} J_{23} - J_{13} J_{22}) \\ + (J_{32} - J_{42})(J_{13} J_{21} - J_{11} J_{23}) \\ + (J_{33} - J_{43})(J_{11} J_{22} - J_{12} J_{21})] = 0. \end{aligned} \tag{B-11}$$

By (B-1), we have

$$\frac{c^2}{\rho_n \alpha_n{}^4 r_{\alpha n}} = - \eta_{11} \eta_{24} - \eta_{13} \eta_{22} . \tag{B-12}$$

Denoting by L_1 the left-hand side of (B-11) and making use of (B-9), (B-10) and (B-12), we find

$$\begin{aligned} L_1 = {} & (\eta_{31} A_{11} + \eta_{33} A_{31} - A_{21} - \eta_{44} A_{41})[\eta_{11}\eta_{24}(A_{22}A_{33} - A_{23}A_{32}) \\ & + \eta_{13}\eta_{22}(A_{13}A_{42} - A_{12}A_{43}) + \eta_{11}\eta_{22}(A_{12}A_{23} - A_{13}A_{22}) \\ & + \eta_{13}\eta_{24}(A_{32}A_{43} - A_{33}A_{42})] + (\eta_{31}A_{12} + \eta_{33}A_{32} - A_{22} - \eta_{44}A_{42}) \\ & \cdot[(\eta_{11}A_{13} + \eta_{13}A_{33})(\eta_{22}A_{21} + \eta_{24}A_{41}) - (\eta_{11}A_{11} + \eta_{13}A_{31})(\eta_{22}A_{23} \\ & + \eta_{24}A_{43})] + (\eta_{31}A_{13} + \eta_{33}A_{33} - A_{23} - \eta_{44}A_{43})[(\eta_{11}A_{11} + \eta_{13}A_{31}) \\ & \cdot(\eta_{22}A_{22} + \eta_{24}A_{42}) - (\eta_{11}A_{12} + \eta_{13}A_{32})(\eta_{22}A_{21} + \eta_{24}A_{41})]. \end{aligned} \tag{B-13}$$

Expanding the above expression and gathering terms, it is found that the coefficients of $\eta_{11}\eta_{22}\eta_{31}$, $\eta_{11}\eta_{22}$, $\eta_{13}\eta_{24}\eta_{33}$, and $\eta_{13}\eta_{24}\eta_{44}$ vanish identically. Using the relations (B-2), (B-3), (B-4), and (B-5), the remaining eight terms, denoted by I_1 through I_8, can be calculated as follows,

$$\begin{aligned} I_1 = {} & \eta_{11}\eta_{22}\eta_{33}[A_{12}A_{23}A_{31} - A_{12}A_{21}A_{33} + A_{11}A_{12}A_{43} \\ & + A_{13}(A_{21}A_{32} - A_{22}A_{31} - A_{11}A_{42})] \\ = {} & \eta_{11}\eta_{12}\eta_{13}A_{12}(A_{23}A_{31} - A_{21}A_{33} + A_{11}A_{43} - A_{13}A_{41}) \\ = {} & 0 \end{aligned}$$

$$I_2 = \eta_{11}\eta_{22}\eta_{44}[A_{11}A_{23}A_{42} - A_{23}A_{32}A_{21} - A_{23}A_{12}A_{41} - A_{22}(A_{11}A_{43} - A_{13}A_{41} - A_{33}A_{21})]$$

$$= \eta_{11}\eta_{2}\eta_{44}A_{23}(A_{11}A_{42} - A_{32}A_{21} + A_{22}A_{31} - A_{12}A_{41})$$

$$= 0$$

$$I_3 = \eta_{11}\eta_{24}\eta_{33}[A_{13}A_{41}A_{32} - A_{11}A_{43}A_{32} - A_{23}A_{32}A_{31} - A_{33}(A_{12}A_{41} - A_{22}A_{31} - A_{11}A_{42})]$$

$$= \eta_{11}\eta_{24}\eta_{33}A_{32}(A_{13}A_{41} - A_{11}A_{43} - A_{23}A_{31} + A_{33}A_{21})$$

$$= 0$$

$$I_4 = \eta_{11}\eta_{24}[A_{12}A_{41}A_{23} - A_{11}A_{42}A_{23} + A_{23}A_{32}A_{21} + A_{22}(A_{11}A_{43} - A_{13}A_{41} - A_{33}A_{21})]$$

$$= \eta_{11}\eta_{24}A_{23}(A_{12}A_{41} - A_{11}A_{4} + A_{32}A_{21} - A_{22}A_{31})$$

$$= 0$$

$$I_5 = \eta_{11}\eta_{24}\eta_{44}[A_{12}A_{41}A_{43} - A_{31}A_{43}A_{22} + A_{21}A_{32}A_{43} + A_{42}(A_{31}A_{23} - A_{33}A_{21} - A_{13}A_{41})]$$

$$= \eta_{11}\eta_{24}\eta_{44}A_{43}(A_{12}A_{41} - A_{31}A_{22} - A_{11}A_{42} + A_{21}A_{32})$$

$$= 0$$

$$I_6 = \eta_{13}\eta_{22}\eta_{31}[A_{31}A_{22}A_{13} - A_{32}A_{21}A_{13} + A_{13}A_{42}A_{11} + A_{12}(A_{33}A_{21} - A_{31}A_{23} - A_{43}A_{11})]$$

$$= \eta_{13}\eta_{22}\eta_{31}A_{13}(A_{31}A_{22} - A_{32}A_{21} + A_{42}A_{11} - A_{12}A_{41})$$

$$= 0$$

$$I_7 = \eta_{13}\eta_{22}\eta_{33}[A_{32}A_{41}A_{13} - A_{31}A_{23}A_{32} - A_{11}A_{43}A_{32} + A_{33}(A_{31}A_{22} - A_{12}A_{41} + A_{11}A_{42})]$$

$$= \eta_{13}\eta_{22}\eta_{33}A_{32}(A_{13}A_{41} - A_{23}A_{31} + A_{21}A_{33} - A_{11}A_{43})$$

$$= 0$$

$$I_8 = \eta_{13}\eta_{22}\eta_{44}[A_{32}A_{21}A_{43} - A_{31}A_{22}A_{43} + A_{12}A_{43}A_{41} + A_{42}(A_{31}A_{23} - A_{21}A_{33} - A_{13}A_{41})]$$

$$= \eta_{13}\eta_{22}\eta_{44}A_{43}(A_{32}A_{21} - A_{22}A_{31} + A_{12}A_{41} - A_{11}A_{42})$$

$$= 0. \tag{B-14}$$

This concludes that $L_1 = 0$ and the equality of $E_{S_i}^{PP}(c)$ and $E_{F_i}^{PP}(c)$ is established.

(2) The second relation of (33) can be established by showing that

$$4\beta_n{}^4 r_{\beta_n}[(J_{31}J_{42} - J_{32}J_{41})p + (J_{31}J_{43} - J_{33}J_{41})q] + \alpha_n{}^4 r_{\alpha_n}[(J_{11}J_{22} - J_{12}J_{21})p + (J_{11}J_{23} - J_{13}J_{21})q] = 0. \tag{B-15}$$

Since the equality

$$(J_{32}J_{41} - J_{31}J_{42}) = -(\alpha_n{}^4 r_{\alpha_n}/4\beta_n r_{\beta_n})(J_{12}J_{21} - J_{11}J_{22}) \tag{B-16}$$

has been shown by Haskell (1962), our problem becomes one of showing

$$4\beta_n{}^4 r_{\beta_n}(J_{31}J_{43} - J_{33}J_{41}) - \alpha_n{}^4 r_{\alpha_n}(J_{11}J_{23} - J_{13}J_{21}) = 0. \tag{B-17}$$

Denoting the left-hand side of (B-17) by L_2 and writing it out explicitly in terms of the elements of A, we have

$$\begin{aligned} L_2 = {} & 4\beta_n{}^4 r_{\beta_n}[\eta_{31}(A_{11}A_{23} - A_{13}A_{21}) + \eta_{31}\eta_{44}(A_{11}A_{43} - A_{13}A_{41}) \\ & + \eta_{33}(A_{31}A_{23} - A_{33}A_{21}) + \eta_{33}\eta_{44}(A_{31}A_{43} - A_{33}A_{41})] \\ & + \alpha_n{}^4 r_{\alpha_n}[\eta_{11}\eta_{22}(A_{11}A_{23} - A_{13}A_{21}) + \eta_{11}\eta_{24}(A_{11}A_{43} - A_{13}A_{41}) \\ & + \eta_{13}\eta_{22}(A_{31}A_{23} - A_{33}A_{21}) + \eta_{13}\eta_{24}(A_{31}A_{43} - A_{33}A_{41})]. \end{aligned} \tag{B-18}$$

By use of the following relations

$$4\beta_n{}^4 r_{\beta_n} \cdot \begin{bmatrix} \eta_{31} \\ \eta_{31}\ \eta_{34} \\ \eta_{33} \\ \eta_{33}\ \eta_{44} \end{bmatrix} = \alpha_n{}^4 r_{\alpha_n} \cdot \begin{bmatrix} -\eta_{11}\ \eta_{22} \\ \eta_{13}\ \eta_{22} \\ \eta_{11}\ \eta_{24} \\ -\eta_{13}\ \eta_{24} \end{bmatrix} \tag{B-19}$$

we rearrange (B-18) and find

$$L_2 = 4\beta_n{}^4 r_{\beta_n}[\eta_{31}(A_{11}A_{23} - A_{13}A_{21} - A_{11}A_{23} + A_{13}A_{21})$$

$$+ \eta_{31}\eta_{44}(A_{11}A_{43} - A_{13}A_{41} + A_{31}A_{23} - A_{33}A_{21})$$

$$+ \eta_{33}(A_{31}A_{23} - A_{33}A_{21} + A_{11}A_{43} - A_{13}A_{41})$$

$$+ \eta_{33}\eta_{44}(A_{31}A_{43} - A_{33}A_{41} - A_{31}A_{43} + A_{33}A_{41})]$$

$$= 0 \qquad \text{(B-20)}$$

from equation (B-5). Therefore, equations (B-16) and (B-20) imply that

$$E_{S_r}^{PSV}(c) = E_{S_r}^{SVP}(c).$$

(**3**) The third relation of (33) is proved following precisely the same steps we have just detailed above in (1). We shall not present the lengthy algebra here, only note that a relation similar to (B-12)

$$\frac{c^2}{4\rho_n \beta_n{}^4 r_{\beta_n}} = -\eta_{33} - \eta_{31}\eta_{44} \qquad \text{(B-21)}$$

is found to be useful.

Acknowledgments

It is a pleasure to thank Professor Don Anderson for reading the manuscript and offering several helpful suggestions. Assistance of Messrs. Laszlo Lenches and John Nordquist in the preparation of graphical materials is acknowledged.

This research was supported by the Air Force Office of Scientific Research, Office of Aerospace Research, United States Air Force, under AFOSR contract number AF-49(638)-1337.

References

Alexander, S. S. and R. A. Phinney (1966). A study of core-mantle boundary using *P*-wave diffracted by the earth's core, *J. Geophys. Res.* **71**, 5943–5958.

Bullen, K. E. (1963). An index of degree of chemical inhomogeneity in the earth, *Geophys. J.* **7**, 584–592.

Dorman, J. (1962). Period equation for waves of Rayleigh type on a layered, liquid-solid half-space, *Bull. Seism. Soc. Am.* **52**, 389–397.

Dorman, J., J. Ewing and L. E. Alsop (1965). Oscillations of the earth: new core-mantle boundary model based on low order free vibrations, *Proc. Nat. Acad. Sci.* **54**, 364–368.

Fernandez, L. M. (1965). The determination of crustal thickness from the spectrum of the *P* wave, *Doctoral Dissertation*, St. Louis University.

Gutenberg, B. (1959). *Physics of the Earth's Interior*, p. 95, Academic Press, New York.

Haskell, N. A. (1953). The dispersion of surface waves in multilayered media, *Bull. Seism. Soc. Am.* **43**, 17–34.

Haskell, N. A. (1960). Crustal reflection of plane *SH* waves, *J. Geophys. Res.* **65**, 4147–4150.

Haskell, N. A. (1962). Crustal reflection of plane *P* and *SV* waves, *J. Geophys. Res.* **67**, 4751–4767.

Kanamori, H. (1966). Spectrum of *P* and *PcP* in relation to the mantle-core boundary and attenuation in the mantle, *J. Geophys. Res.*, **72**, 559–571.

Landisman, M., Y. Satô and J. Nafe (1965). Free vibration of the earth and the properties of its deep interior regions, Part 1: Density, *Geophys. J.* **9**, 469.

Phinney, R. A. (1964). Structure of the earth's crust from spectral behavior of long-period body waves, *J. Geophys. Res.* **69**, 2997–3017.

Phinney, R. A. and S. S. Alexander (1966). Diffraction of *P* waves and the structure of the core mantle boundary, *J. Geophys. Res.* **71**, 5959–5975.

Seismological Laboratory
California Institute of Technology
Pasadena, California
(Division of Geological Sciences Contribution No. 1430)

Manuscript received November 14, 1966.